

Enhancing Supervised Composed Image Retrieval via Reasoning-Augmented Representation Engineering

Jun Li*, Kai Li*, Shaoguo Liu[†], Tingting Gao

Kuaishou Technology

Abstract

Composed Image Retrieval (CIR) presents a significant challenge as it requires jointly understanding a reference image and a modified textual instruction to find relevant target images. Some existing methods attempt to use a two-stage approach to further refine retrieval results. However, this often requires additional training of a ranking model. Despite the success of Chain-of-Thought (CoT) techniques in reducing training costs for language models, their application in CIR tasks remains limited—compressing visual information into text or relying on elaborate prompt designs. Besides, existing works only utilize it for zero-shot CIR, as it is challenging to achieve satisfactory results in supervised CIR with a well-trained model. In this work, we proposed a framework that includes the **Pyramid Matching Model with Training-Free Refinement (PMTFR)** to address these challenges. Through a simple but effective module called **Pyramid Patcher**, we enhanced the Pyramid Matching Model’s understanding of visual information at different granularities. Inspired by representation engineering, we extracted representations from COT data and injected them into the LVLMs. This approach allowed us to obtain refined retrieval scores in the Training-Free Refinement paradigm without relying on explicit textual reasoning, further enhancing performance. Extensive experiments on CIR benchmarks demonstrate that PMTFR surpasses state-of-the-art methods in supervised CIR tasks. The code will be made public.

Introduction

In recent years, Composed Image Retrieval (CIR) (Vo et al. 2019a; Goenka et al. 2022; Wen et al. 2023; Bai et al. 2024) has gained increasing attention. Compared to traditional image retrieval tasks (Gordo et al. 2016; Liu et al. 2016; Chen et al. 2022), CIR requires not only a reference image as input but also a textual description of the expected modifications to the reference image. The complexity of understanding multi-modal data and modeling cross-modal relationships presents technical challenges, but also enables novel applications of CIR methods in fields such as e-commerce (Shankar et al. 2017) and Internet search (Deldjoo et al. 2023).

Large Vision-Language Models (LVLMs) have demonstrated promising multimodal understanding capabilities,

*These authors contributed equally.

[†]Corresponding author

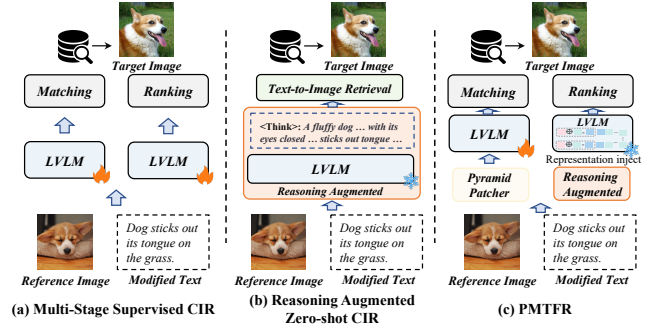


Figure 1: Comparison of Different Training Paradigms. (a) The Multi-stage supervised method requires additional training of a ranking model. (b) Utilizing the LVLMs to generate better reasoning text descriptions (Reasoning-Augmented) for zero-shot CIR tasks through a training-free approach. (c) The proposed PMTFR utilizes Pyramid Patcher to capture richer visual information and benefits the model in a training-free manner through the representation injection of the reasoning-augmented information.

and have been adopted in various multimodal tasks, including visual grounding (Deng et al. 2021), visual question answering (Antol et al. 2015), and CIR tasks (Bai et al. 2024; Sun et al. 2025; Karthik et al. 2024; Sun, Ye, and Gong 2023). However, some of these works (Karthik et al. 2024; Tang et al. 2025b) use LVLMs to extract better textual descriptions, which are then used to retrieve images, while others (Sun et al. 2025; Bai et al. 2024) rely on complex input prompt designs. These cross-modal generation—such as image captioning—inevitably leads to information loss. For that sake, these methods may fall short in CIR tasks which require both multi-granular visual information and cross-modal correlation understanding. For example, given the modified instruction ‘dog sticks out its tongue on the grass’ (in Fig. 1), the CIR models need to consider both macro-level background information ‘on the grass’ and micro-level details of the dog’s tongue.

Based on these considerations, we propose training a Pyramid Matching Model by utilizing a pre-trained LVLm. By removing the large language model (LLM) head and taking the last token as representation, we simply input com-

posed queries and target images, and use InfoNCE (He et al. 2020) loss to minimize the distance between positive pairs while maximizing the distance between negative pairs. This approach allows for better utilization of the world knowledge embedded in the pre-trained LVLM, while quickly adapting to the CIR task through straightforward alignment training. To enhance the model’s understanding of both fine-grained and coarse-grained visual information, we propose a module named Pyramid Patcher, inspired by the multi-scale technique in visual detection (Singh and Davis 2018). Unlike the multi-scale technique, which randomly introduces images of different scales during training to adapt to varying object sizes during testing, Pyramid Patcher divides an image into multiple tokens with different visual receptive fields. This approach significantly improves the capability of LVLM without introducing excessive computational overhead. After training the Pyramid Matching Model, we can obtain an initial retrieval result for any composed query.

In supervised CIR tasks, the retrieval model is required to be trained on a training set within a specific domain and tested within it to evaluate performance. Some existing multi-stage methods (Liu et al. 2023b, 2025) additionally train a ranking model to reorder the retrieval results for more accurate results. However, training a ranking model requires reconstructing the training data and consumes additional computational resources. This leads us to consider *whether it is possible to refine retrieval results without training*. Achieving this without training while providing informational gain often implies a stronger generalization ability. This directs our attention to Chain-of-Thought (Wei et al. 2022), which can enhance the capabilities of models without additional training. In zero-shot CIR tasks (Yang et al. 2024), some methods (Sun, Ye, and Gong 2023; Tang et al. 2025b) incorporate the Chain-of-Thought to generate more accurate textual descriptions of reference images and modified instructions. After that, these methods utilized the CLIP (Radford et al. 2021) model for text and image representation extraction to perform retrieval. Based on these considerations, we designed a Training-Free Refinement paradigm, which adjusts the retrieval results of the Pyramid Matching Model, without the need to train an additional ranking model, thus achieving further performance improvements.

However, directly adopting such Reasoning methods presents two problems: 1) In zero-shot CIR tasks, these methods aim to produce better textual descriptions, while in our Training-Free Refinement stage, we aim to obtain a better refinement score. 2) Existing reasoning-based methods rely on explicit textual reasoning paths, which often lead to significant consumption of computing resources. To address these empirical research gaps, we first pair the composed query with the candidate images retrieved by the Pyramid Matching Model, then utilize the pre-trained LVLM to determine whether they form a correct combination to obtain a refinement score. Inspired by representation engineering (Tang et al. 2025a; Zou et al. 2023), which extracted the representations of LLMs with data that reflects specific capabilities, and treats these representations as the fundamental unit of analysis to understand and control high-level

capabilities of LLMs. We designed a reasoning-augmented representation (RAug-Rep) extraction and injection method in the Training-Free Refinement stage. On the training set, we extract the ‘RAug-Rep’ using pre-generated reasoning paths. During the inference phase, we inject the ‘RAug-Rep’ into the intermediate layers of the model to participate in the forward propagation of model. Interestingly, this approach effectively improves the accuracy of the refinement scores, as if finding a key to unlock a certain capability of the model. By simply inserting it into the model, we can stimulate a certain capability of the model, thereby achieving a performance improvement without inputting any explicit textual reasoning paths. Our main contributions are summarized as follows:

- We proposed a novel framework that includes the **Pyramid Matching Model with Training-Free Refinement (PMTFR)**, which enhances the model’s understanding of both coarse-grained and fine-grained visual information and employs a novel training-free paradigm to further refine the retrieval results.
- To the best of our knowledge, we are the first to apply representation engineering to the CIR task by extracting representations from reasoning paths and injecting them into the model, which provides an interesting direction for exploration within the CIR community.
- We propose the Pyramid Patcher module, which is simple yet quite effective. It provides the model with tokens of different visual receptive fields and leads to performance improvements.
- Extensive experiments are conducted on two commonly used benchmarks, which demonstrate that PMTFR outperforms all the state-of-the-art methods in supervised CIR tasks.

Related Works

Composed Image Retrieval

Composed Image Retrieval (CIR) (Vo et al. 2019a) is a challenging task due to its reliance on multimodal information for target image retrieval. Most works focus on how to better integrate multimodal information, such as early-fusion (Wen et al. 2024; Levy et al. 2024) and late-fusion (Baldrati et al. 2022; Chen, Zhou, and Peng 2024). Some methods (Liu et al. 2023b, 2025) employ a multi-stage paradigm, where a ranking model is trained in the second stage to further enhance retrieval performance. However, training a ranking model requires reconstructing the training data and consumes additional computational resources. With the rapid development of Chain-of-Thought (Wei et al. 2022), many works (Sun, Ye, and Gong 2023; Tang et al. 2025b; Yang et al. 2024) utilize this technique in zero-shot CIR tasks to generate better text descriptions. Nevertheless, these reasoning-augmented texts depend on complex prompt designs and explicit reasoning paths, posing significant challenges for implementation in embedding-based retrieval tasks like supervised CIR. Based on this, we propose the PMTFR, which combines the advantages of multi-stage and reasoning-augment, achieving better performance with higher efficiency.

Large Vision-Language Models

Large Vision-Language Models (LVLMs) have made significant strides in multimodal learning, such as BLIP (Li et al. 2022), LLaVA (Liu et al. 2023a), and Qwen-VL (Bai et al. 2023). The LVLMs have achieved excellent results in various multimodal tasks, including visual grounding (Deng et al. 2021) and visual question answering (Antol et al. 2015), among others. In recent years, some CIR methods (Sun et al. 2025; Bai et al. 2024; Li et al. 2025) have started leveraging the capabilities of LVLMs. They use LVLMs to enhance model performance by generating better textual descriptions (Tang et al. 2025b), sentence-level prompting (Bai et al. 2024), or soft prompting (Sun et al. 2025). These works mostly focus on complex designs for text, thereby overlooking the exploration of rich visual cues. In contrast, we leverage the LVLM as an encoder, simply inputting the composite query and target image to obtain the corresponding representations. To enhance the understanding of visual information, we propose a straightforward Pyramid Patcher module, which enables the model to handle information at different visual granularities.

Representation Engineering

Representation Engineering (RepE) (Zou et al. 2023) extracted the representations of large language models (LLMs) with data that reflects specific capabilities, and treats these representations as the fundamental unit of analysis to understand and control high-level capabilities of LLMs. As a widely applied technology, it is often used in LLMs and applied in many areas, such as hallucination alleviation (Arditi et al. 2024; Li et al. 2023), instruction following (Stolfo et al. 2024), and reasoning (Tang et al. 2025a). In recent years, there have also been works (Tian et al. 2025a; McGrath et al. 2022) beginning to explore its potential applications in LVLMs. In this work, we pioneer the adaptation of RepE to composed image retrieval (CIR), where reasoning-augmented representations are extracted and injected via a training-free paradigm to boost retrieval performance significantly.

Method

Preliminary

Task definition. Composed image retrieval (CIR) is a multimodal retrieval task that aims to retrieve the correct target image from a pool of candidate images based on a reference image and its corresponding modified text. Specifically, the composed query is denote as $\mathcal{Q}_i = \{\mathbf{I}_i^r, \mathbf{T}_i\}$, where \mathbf{I}_i^r denotes the reference image, and \mathbf{T}_i denotes the modified text. The goal of the CIR task is to retrieve the correct target image \mathbf{I}_i^t from the candidate set $\mathcal{D} = \{\mathbf{I}_0^t, \mathbf{I}_1^t, \dots, \mathbf{I}_{C-1}^t\}$.

PMTR

PMTR consists of the Pyramid Matching Model and Training-Free Refinement as shown in Fig. 2. In the Pyramid Matching Model, the model learn a general representation of multimodal queries and images through a concise contrastive learning paradigm, which facilitates rapid retrieval. To enhance the model’s understanding of

multi-granular visual information, we propose a module named Pyramid Patcher that provides the model with visual tokens of different receptive fields, substantially improving the capability of model. Inspired by representation engineering, we extracted representations from Chain-of-Thought data and injected them into the Training-Free Refinement.

Pyramid Patcher. In a standard Vision Transformer (ViT) (Dosovitskiy et al. 2021), an input 2D image $\mathbf{I} \in \mathbb{R}^{H \times W \times C}$ is divided into patches, resulting a sequence of flattened 2D patches $\mathbf{I}^p \in \mathbb{R}^{L \times (P^2 \cdot C)}$, where (H, W) is the resolution of the original image, C is the number of channels, P is the patch size and $L = HW/P^2$. The final token sequence fed into the visual encoder can be formulated as:

$$\mathbf{I}^e \in \mathbb{R}^{L \times D} = \text{Emb}(\mathbf{I}^p), \quad (1)$$

where D denotes the dimension of the visual encoder, $\text{Emb}(\cdot)$ denotes the embedding layers. In order to enhance the model’s understanding of multi-granular visual information, we propose the Pyramid Patcher that provides the model with visual tokens of different receptive fields. To simultaneously obtain Tokens with M different visual scales, we first duplicate the image M times, i.e. $\mathcal{S} = \{\mathbf{I}_0, \mathbf{I}_1, \dots, \mathbf{I}_{M-1}\}$. We use a patch size of P for the \mathbf{I}_0 , $2 \times P$ for the \mathbf{I}_1 and $2^{M-1} \times P$ for the \mathbf{I}_{M-1} . So the flattened 2D patches set can be formulated as:

$$\mathcal{S}^p = \left\{ \mathbf{I}_i^p \in \mathbb{R}^{\frac{L}{2^i} \times (2^i \cdot P^2 \cdot C)} \mid i \in \mathbb{Z}, 0 \leq i < M \right\}, \quad (2)$$

where L is the number of visual tokens in the original image \mathbf{I}_0 . The final multi-scale visual tokens can be formulated as:

$$\begin{aligned} \mathbf{I}_M^e &= \text{cat}[\{\text{Emb}(\mathbf{I}_i^p) \mid \mathbf{I}_i^p \in \mathcal{S}^p\}] \\ &= \text{cat} \left[\left\{ \mathbf{I}_i^e \in \mathbb{R}^{\frac{L}{2^i} \times D} \mid i \in \mathbb{Z}, 0 \leq i < M \right\} \right], \end{aligned} \quad (3)$$

where the $\text{cat}[\cdot]$ denotes the concatenation operation performed along the first dimension. After processing with Pyramid Patcher, for a visual token in \mathbf{I}_0^e and \mathbf{I}_{M-1}^e , the former will contain more detailed visual information, while the latter will contain more macroscopic visual information.

Pyramid Matching Model. The training objective of the model is to align the representations of the composed queries $\mathcal{Q} = \{\mathbf{I}^r, \mathbf{T}\}$ with the representations of the target images \mathbf{I}^t . For the model $f_\theta(\cdot)$, we take the hidden states of the last token as the representation, which can be formulated as:

$$\begin{aligned} \mathbf{u}^q &= f_\theta(f_\zeta(\mathbf{I}_r), \mathbf{T}) \\ \mathbf{u}^t &= f_\theta(f_\zeta(\mathbf{I}_t)), \end{aligned} \quad (4)$$

where $f_\zeta(\cdot)$ denotes the Pyramid Patcher. For a sample pair $\langle \mathbf{u}^q, \mathbf{u}^t \rangle$, we use the InfoNCE (He et al. 2020) loss to minimize the similarity between the positive pairs and maximize between the negative pairs. Specifically, let N denote the size of the mini-batch and denote Ψ the set of all target image representations in a mini-batch, then the loss function can be expressed as:

$$L = \sum_i^N -\log \left(\frac{\exp(\mathbf{u}_i^q \mathbf{u}_i^t / \tau)}{\sum_{\mathbf{u}_j^t \in \Psi} \exp(\mathbf{u}_i^q \mathbf{u}_j^t / \tau)} \right), \quad (5)$$

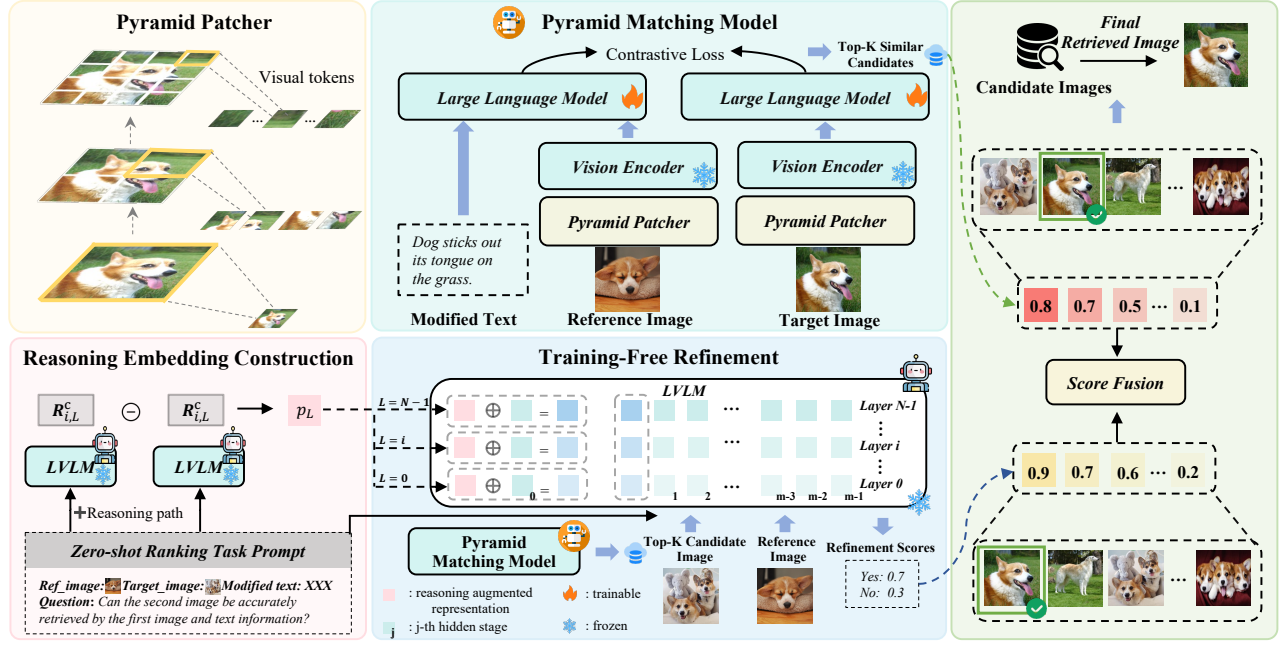


Figure 2: Overall pipeline of the proposed PMTFR. PMTFR is essentially a two-stage approach. In the first stage, the Pyramid Matching Model is used to obtain an initial retrieval result, where the Pyramid Patcher acquires tokens with different visual receptive fields for the visual input. The second stage is Training-Free Refinement, where representations are extracted from the reasoning data and then injected into the model. After that, we obtain more accurate correction scores, which are then fused with the scores from the initial retrieval result to serve as the basis for ranking.

where τ is a temperature hyper-parameter. During validation, for any composed query, we select the Top-N of the retrieval result according to the similarity score, where s_i^m denotes the score of retrieval result x_i .

Reasoning-Augmented Representation Construction. Recent works such as DeepSeek-R1 (Guo et al. 2025) have demonstrated the surprising generalization capabilities of Chain-of-Thought (COT) (Wei et al. 2022) across many tasks. However, this ability relies on explicit textual reasoning, which is not naturally compatible with embedding-based retrieval approaches such as CIR. Fortunately, with the help of representation engineering (Zou et al. 2023), we extract an ‘RAug-Rep’ that benefits from the reasoning ability of the model and enables model performance gains. Specifically, for a positive pair $\langle Q_i, \tilde{I}_i^t \rangle$ in the training set, we first use the ‘Refinement Prompt’ (see Appendix A) to construct the question q_i . We then employ the ‘Reasoning Path Construction Prompt’ (see Appendix A) to generate input for GPT-4o (Hurst et al. 2024), obtaining the reasoning path denoted as c_i . For each of these inputs, we feed them separately into the pre-trained LVLM to extract layer-wise representations. Formally, for the standalone question q_i and the augmented input $(q_i; c_i)$ (where $;$ denotes concatenation), the corresponding representations can be formulated as:

$$R_{i,L}^q = h_L^{-1}(q_i) \quad R_{i,L}^c = h_L^{-1}(q_i; c_i), \quad (6)$$

where $h_L^{-1}(s)$ denotes the hidden states corresponding to the last token in the token sequence s at the layer L in LLM. We take the $R_{i,L}^c - R_{i,L}^q$ as the ‘RAug-Rep’ and average it over all samples in the training set, which can be formulated as:

$$p_L = \frac{1}{|\Phi|} \sum_{i=1}^{|\Phi|} (R_{i,L}^c - R_{i,L}^q), \quad (7)$$

where Φ denotes all the samples in the training set.

Training-Free Refinement. In the Training-Free Refinement, we inject ‘RAug-Rep’ into a pre-trained LVLM to get the refinement score of the pair $\langle Q_i, x_i \rangle$, where Q_i denotes the composed query in the validation set and x_i denotes one of the Top-N images retrieved by the Pyramid Matching Model. For the pair $\langle Q_i, x_i \rangle$, we use the Refinement prompt (more details in Appendix) to form the question q'_i , and the ‘RAug-Rep’ will be injected into certain layers of the model. We input q'_i to a pre-trained LVLM to get the probability (i.e., refinement score) of the [YES] token. For more discussions on the selection of layers, please refer to Tab. 4. For a specific layer L in the language model, we add the ‘RAug-Rep’ of the corresponding layer to the first token of the hidden states in that layer:

$$\tilde{h}_L^0 = h_L^0 + \alpha \cdot p_L, \quad (8)$$

where h_L^0 denotes the 0th token of the hidden states in layer L and α is the hyperparameter to balance the strength of

Method	Ref.	Shirt		Dress		Tops&Tees		Avg.		
		R@10	R@50	R@10	R@50	R@10	R@50	R@10	R@50	R_{mean}
TIRG	CVPR'19	13.10	30.91	14.13	34.61	14.79	34.37	14.01	33.30	23.66
ARTEMIS	ICLR'22	21.57	44.13	25.68	51.05	28.59	55.06	25.28	50.08	37.68
TG-CIR	MM'23	52.60	72.52	45.22	69.66	56.14	77.10	51.32	73.09	62.16
BLIP4CIR+Bi	WACV'24	41.76	64.28	42.09	67.33	46.61	70.32	43.49	67.31	55.40
Re-ranking	TMLR'24	50.15	71.25	48.14	71.34	55.23	76.80	51.17	51.17	62.15
CASE	AAAI'24	48.48	70.23	47.44	69.36	50.18	72.24	48.79	70.68	59.74
SPRC	ICLR'24	55.64	73.89	49.18	72.43	59.35	78.58	54.92	74.97	64.85
CCIN	CVPR'25	55.93	74.14	49.38	72.58	57.93	77.56	54.41	74.76	64.59
CIR-LVLM	AAAI'25	<u>58.59</u>	<u>75.86</u>	50.42	73.57	59.61	78.99	56.21	76.14	66.17
ENCODER	AAAI'25	54.86	74.93	<u>51.51</u>	76.95	62.01	80.88	<u>56.13</u>	77.59	<u>66.86</u>
PMTFR		59.33	76.13	53.63	<u>75.47</u>	<u>60.63</u>	<u>80.32</u>	57.86	<u>77.31</u>	67.59

Table 1: Comparison with the state-of-the-art methods on the validation set of Fashion-IQ, where R_{mean} indicates the average results across all the metrics. The best results are in **boldface**, while the second-best results are underlined.

injection. After that, following (Liu et al. 2024a), we scaled the magnitude of the vectors back to their original scale:

$$\hat{h}_L^0 = \tilde{h}_L^0 \cdot \frac{\|h_L^0\|_2}{\|\tilde{h}_L^0\|_2}. \quad (9)$$

We use the probability that the model outputs [YES] as the refinement score, denoted as s_i^r . Finally, for each retrieval candidate, the final score can be formulated as:

$$s_i = \lambda s_i^r + (1 - \lambda) s_i^m, \quad (10)$$

where λ is the refinement strength. We use the final scores s_i as the basis for sorting the final retrieval results.

Experiments

Datasets and Metrics

Following SPRC (Bai et al. 2024), we have selected the two most commonly used benchmarks for the supervised CIR task: Fashion-IQ (Wu et al. 2021) and CIR (Liu et al. 2021). (1) **Fashion-IQ** comprises 77,684 fashion images, which are carefully organized into 30,134 triplets and categorized into three distinct subsets: Dress, Shirt, and Tootie. Following previous work (Bai et al. 2024; Sun et al. 2025), we trained our model on the training set and reported the Recall@K metrics for three subsets on the validation set. (2) **CIRR** is a general image dataset that comprises 36,554 triplets. Following previous work (Bai et al. 2024; Liu et al. 2021), we trained our model in the training set and performed hyperparameter selection on the validation set. Finally, we submitted the prediction results of the test set to an online server to obtain the Recall@K metrics on the entire set and subsets.

Implementation Details

We used the pre-trained Qwen2-VL-7B (Bai et al. 2023) model to initialize the weights of the Pyramid Matching Model and employed the AdamW optimizer, with a learning rate set to 4e-5 for 2 epochs. The temperature in InfoNCE was set to 0.005, with a batch size of 1024 for the Fashion-IQ dataset and 512 for the CIRR dataset. N is set

to 100 in the selection of the top N candidates. The pre-trained Qwen2-VL-7B is used in the Training-Free Refinement. All hyperparameters were selected using the validation set and held constant across experiments. All hyperparameter selections were made on the validation set and applied to all experiments. All experiments were conducted on a single NVIDIA A800 machine.

Experimental Results

To evaluate the superiority of PMTFR, we compare our work with established baselines such as TIRG (Vo et al. 2019b), ARTEMIS (Delmas et al. 2022), TG-CIR (Wen et al. 2023), SPRC (Bai et al. 2024), bi (Liu et al. 2024b), CASE (Levy et al. 2024), DWC (Huang et al. 2024) and FashionERN (Chen et al. 2024), multi-stage work including Re-ranking (Liu et al. 2023b), as well as with the latest accepted works, including CIR-LVLM (Sun et al. 2025), Encoder (Li et al. 2025), CCIN (Tian et al. 2025b).

Comparisons to Prior Arts. As reported in Tab. 1 and Tab. 2, PMTFR outperformed previous methods in terms of average recall metrics on both the Fashion-IQ and CIRR datasets. Traditional methods based on ResNet, such as TIRG and ARTEMIS, performed significantly worse compared to many recent methods based on LVLMs. Compared to CIR-LVLM, which also utilizes LVLMs, our approach outperformed it across all 9 metrics on the Fashion-IQ dataset, achieving an average improvement of **1.42%**. Similarly, on the CIRR dataset, our method surpassed CIR-LVLM in all 7 metrics, with an average gain of **1.22%**. In addition, unlike CIR-LVLM, which introduced task prompts and soft prompts that occupy excessive input context length, our method only utilized modified text and image information as input, which ensured higher training efficiency. Notably, compared to the two-stage Re-ranking method, our method achieved an average improvement of **5.44%** on the Fashion-IQ dataset and **1.76%** on the CIRR dataset, without additional training of ranking model. These results further demonstrate the superiority of our proposed method.

Method	Ref.	Recall@K				Recall _{subset} @K			Avg.
		K=1	K=5	K=10	K=50	K=1	K=2	K=3	
TIRG	CVPR'19	14.61	48.37	64.08	90.03	—	—	—	—
ARTEMIS	ICLR'22	16.96	46.10	61.31	87.73	39.99	62.20	75.67	43.05
TG-CIR	MM'23	45.25	78.29	87.16	97.30	72.84	89.25	95.13	75.57
BLIP4CIR+Bi	WACV'24	40.15	73.08	83.88	96.27	72.10	88.27	95.93	72.59
Re-ranking	TMLR'24	50.55	81.75	89.78	97.18	80.04	91.90	96.58	80.90
CASE	AAAI'24	48.00	79.11	87.25	97.57	75.88	90.58	96.00	77.50
SPRC	ICLR'24	51.96	82.12	89.74	97.69	80.65	92.31	96.60	81.38
CCIN	CVPR'25	53.41	<u>84.05</u>	91.17	<u>98.00</u>	—	—	—	—
ENCODER	AAAI'25	46.10	77.98	87.16	97.64	76.92	90.41	95.95	77.45
CIR-LVLM	AAAI'25	<u>53.64</u>	83.76	90.60	97.93	79.12	<u>92.33</u>	<u>96.67</u>	<u>81.44</u>
PMTFR		55.01	84.72	<u>91.06</u>	98.58	<u>80.60</u>	92.75	96.84	82.66

Table 2: Comparison with the state-of-the-art methods on the test set of CIRR, where Avg. indicates the average results of Recall@5 and Recall_{subset}@1. The best results are in **boldface**, while the second-best results are underlined.

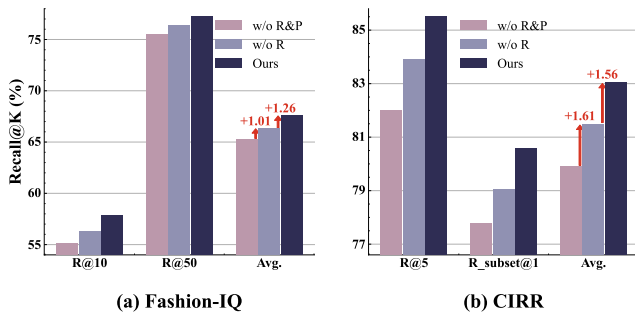


Figure 3: Ablation on Pyramid Patcher (denoted as P) and Training-Free Refinement (denoted as R).

M	R@10	R@50	R_{mean}	Token Length
1	55.15	75.49	65.32	165
2	55.54	75.19	65.37	213
3	55.35	75.86	65.60	225
4	55.37	75.91	65.64	229
5	56.30	76.36	66.33	231

Table 3: Comparison to different M of Pyramid Patcher in matching stage.

Ablation Study & Analysis

Effect of Pyramid Patcher and Training-Free Refinement. In Fig. 3, we conducted ablation experiments on Pyramid Patcher and Training-Free Refinement in the validation sets of Fashion-IQ and CIRR, and both parts provide notable performance gains. Pyramid Patcher brings an average metric improvement of **1.01%** in the Fashion-IQ dataset and **1.61%** in the CIRR dataset. Training-Free Refinement further delivers an average metric improvement of **1.26%** in the Fashion-IQ and **1.56%** in the CIRR. A more detailed analysis of both parts will be presented later.

Different visual scales of Pyramid Patcher. As shown in Eq. 2, the number of visual levels is denoted by M in Pyramid Patcher. We conducted experiments on Fashion-IQ

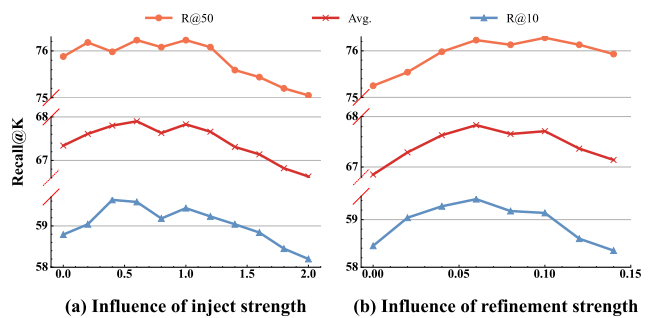


Figure 4: Sensitivity Analysis of different (a) inject strength α and (b) refinement strength λ in Training-Free Refinement on the validation set of Fashion-IQ shirt.

using different M and reported the corresponding recall metrics and number of image Tokens. As shown in Tab. 3, larger M can obtain more diverse visual receptive field tokens and achieve better performance. Since a larger patch size results in fewer image tokens, the number of image tokens does not increase significantly with the increase in M . Compared to not using Pyramid Patcher ($M = 1$), we achieved an improvement of **1.01%** when $M = 5$. Finally, we chose the M of 5 as the default setting.

Sensitivity Analysis. We further analyze the contributions of Training-Free Refinement on Fashion-IQ shirt, examining two key hyperparameters: representation injection strength (α) in Eq. 8, and refinement score weighting (λ) in Eq. 10. As shown in Fig 4 (a), model performance improves significantly with moderate injection of ‘RAug-Rep’. This indicates that these representations derived from explicit reasoning paths contain valuable information that activates latent model capabilities. However, excessive injection strength disrupts the original input distribution, degrading performance due to representation misalignment. The $\alpha = 0.6$ brings the best performance, which is set to the default configuration for all experiments in this work. Regarding the refinement strength, the best performance

Inject Pos.	R@10	R@50	R_{mean}
First	58.64	75.49	67.07
Middle	58.89	75.69	67.29
Last	58.74	75.69	67.22
All	59.33	76.13	67.73

Table 4: Comparison to different inject positions of ‘RAug-Rep’ in the Training-Free Refinement.

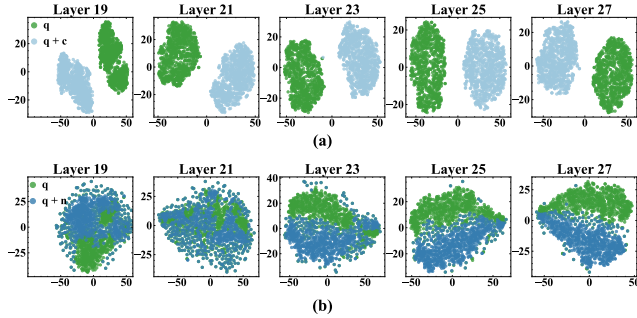


Figure 5: Visualization of the distribution of the last token from different layers using t-SNE. (a) inputting only the question (denoted as q) and the question along with the reasoning path (denoted as $q + c$); (b) inputting only the question (denoted as q) and the question along with the noise text (denoted as $q + n$).

was achieved at 0.06 as shown in Fig 4 (b). Interestingly, even with a very small refinement strength (0.06) applied to adjust the matching scores, the average recall metric improved by **0.98%**. This demonstrates the effectiveness of the Training-Free Refinement.

Different inject position in Training-Free Refinement.

When extracting ‘RAug-Rep’, we capture layer-specific features to enable flexible injection position. We empirically evaluated injection strategies on the Fashion-IQ shirt validation set using four configurations: **First** (Layer-0), **Middle** (Layer-14), **Last** (Layer-27), and **All** (Layer-0~27). From the Tab. 4, first-layer injection demonstrates a limited impact compared to middle/last-layer injection. We hypothesize this occurs because the injected representation attenuates during forward diminishes through subsequent transformer layers. Full-layer injection achieved optimal performance, indicating that single-layer modifications provide insufficient refinement. Consequently, we adopt all-layer injection as the default configuration across all experiments.

Visualization of representation. As shown in Fig. 5 (a), we visualized the $R_{i,L}^q(q)$ and $R_{i,L}^c(q + c)$ mentioned in Eq. 6 using the t-SNE (Maaten and Hinton 2008) and selected the last several layers for display. Meanwhile, we replaced the reasoning path with noisy text ($q + n$), and illustrated its distribution in Fig. 5 (b). It can be observed that inputs containing richer informational content (reasoning paths) yield representations with greater distributional divergence from the original. This indicates

Method	Training	Inference	Tot.	R@10	R@50
TR	2.3h / epoch	0.3h	2.6h	59.28	76.38
TFR	–	0.3h	0.3h	59.33	76.13

Table 5: The time consumption and recall metrics of different training paradigms in the second stage. TR is short for Training Ranking model, TFR is short for Training-Free Refinement.

that the information density of inputs manifests in their representation distributions. Based on these, during the reasoning-augmented representation Construction phase, we used the $R_{i,L}^c - R_{i,L}^q$ as the final ‘RAug-Rep’. The aim is to utilize this difference as a medium, allowing the model to acquire approximate capabilities without depending on explicit reasoning paths.

Efficiency of the Training-Free Refinement. We conduct experiments on the Fashion-IQ shirt dataset to compare the efficiency and effectiveness of training a ranking model (denoted as TR) versus Training-Free Refinement (denoted as TFR). While keeping the Matching Model unchanged, we constructed a dataset for ranking training using the top 10 recall results and trained a ranking model to sort these recall results. In contrast, the Training-Free Refinement does not need any training. As shown in Tab. 5, Training-Free Refinement can significantly reduce the time consumption while achieving results close to those of retraining the ranking model, demonstrating the effectiveness of the Training-Free Refinement.

Conclusions and limitations

In this work, we propose the Pyramid Matching Model with Training-Free Refinement (PMTFR). By incorporating the Pyramid Patcher module, our model effectively captures both fine-grained and coarse-grained visual information, leading to performance improvement. The Training-Free Refinement paradigm, which utilizes ‘RAug-Rep’ extraction and injection, allows for refinement of retrieval results without the need for additional training. While extensive experiments on widely-used benchmarks demonstrate that PMTFR outperforms existing state-of-the-art methods in supervised CIR tasks, there are still some limitations. Although t-SNE visualization revealed that the representation distributions with and without Chain-of-Thought data form two clusters, there may be other reasonable methods worth exploring beyond simply subtracting the two representations. The ‘RAug-Rep’ is extracted and benefited from Chain-of-Thought data, and interestingly, they achieved performance improvements with generalization capabilities. However, the specific mechanisms at play and their connection to the reasoning abilities of model are complex and were not deeply discussed in this work. This remains a promising research direction that we hope will inspire future studies.

References

- Antol, S.; Agrawal, A.; Lu, J.; Mitchell, M.; Batra, D.; Zitnick, C. L.; and Parikh, D. 2015. VQA: Visual Question Answering. In *Proc. of ICCV*, 2425–2433.
- Arditi, A.; Obeso, O.; Syed, A.; Paleka, D.; Panickssery, N.; Gurnee, W.; and Nanda, N. 2024. Refusal in Language Models Is Mediated by a Single Direction. In *Proc. of NeurIPS*.
- Bai, J.; Bai, S.; Yang, S.; Wang, S.; Tan, S.; Wang, P.; Lin, J.; Zhou, C.; and Zhou, J. 2023. Qwen-vl: A frontier large vision-language model with versatile abilities. *ArXiv preprint*.
- Bai, Y.; Xu, X.; Liu, Y.; Khan, S.; Khan, F.; Zuo, W.; Goh, R. S. M.; and Feng, C. 2024. Sentence-level Prompts Benefit Composed Image Retrieval. In *Proc. of ICLR*.
- Baldrati, A.; Bertini, M.; Uricchio, T.; and Bimbo, A. D. 2022. Conditioned and composed image retrieval combining and partially fine-tuning CLIP-based features. In *Proc. of CVPR*, 4955–4964.
- Chen, W.; Liu, Y.; Wang, W.; Bakker, E. M.; Georgiou, T.; Fieguth, P.; Liu, L.; and Lew, M. S. 2022. Deep learning for instance retrieval: A survey. *IEEE Transactions on Pattern Analysis and Machine Intelligence*, 7270–7292.
- Chen, Y.; Zhong, H.; He, X.; Peng, Y.; Zhou, J.; and Cheng, L. 2024. FashionERN: Enhance-and-Refine Network for Composed Fashion Image Retrieval. In *Proc. of AAAI*, 1228–1236.
- Chen, Y.; Zhou, J.; and Peng, Y. 2024. Spirit: Style-guided patch interaction for fashion image retrieval with text feedback. *ACM Transactions on Multimedia Computing, Communications and Applications*, 1–17.
- Deldjoo, Y.; Nazary, F.; Ramisa, A.; Mcauley, J.; Pellegrini, G.; Bellogin, A.; and Noia, T. D. 2023. A review of modern fashion recommender systems. *ACM Computing Surveys*, 1–37.
- Delmas, G.; de Rezende, R. S.; Csurka, G.; and Larlus, D. 2022. ARTEMIS: Attention-based Retrieval with Text-Explicit Matching and Implicit Similarity. In *Proc. of ICLR*.
- Deng, J.; Yang, Z.; Chen, T.; Zhou, W.; and Li, H. 2021. TransVG: End-to-End Visual Grounding with Transformers. In *Proc. of ICCV*, 1749–1759.
- Dosovitskiy, A.; Beyer, L.; Kolesnikov, A.; Weissenborn, D.; Zhai, X.; Unterthiner, T.; Dehghani, M.; Minderer, M.; Heigold, G.; Gelly, S.; Uszkoreit, J.; and Hounsby, N. 2021. An Image is Worth 16x16 Words: Transformers for Image Recognition at Scale. In *Proc. of ICLR*.
- Goenka, S.; Zheng, Z.; Jaiswal, A.; Chada, R.; Wu, Y.; Hedau, V.; and Natarajan, P. 2022. FashionVLP: Vision Language Transformer for Fashion Retrieval with Feedback. In *Proc. of CVPR*, 14085–14095.
- Gordo, A.; Almazán, J.; Revaud, J.; and Larlus, D. 2016. Deep image retrieval: Learning global representations for image search. In *Proc. of ECCV*, 241–257.
- Guo, D.; Yang, D.; Zhang, H.; Song, J.; Zhang, R.; Xu, R.; Zhu, Q.; Ma, S.; Wang, P.; Bi, X.; et al. 2025. Deepseek-r1: Incentivizing reasoning capability in llms via reinforcement learning. *ArXiv preprint*.
- He, K.; Fan, H.; Wu, Y.; Xie, S.; and Girshick, R. B. 2020. Momentum Contrast for Unsupervised Visual Representation Learning. In *Proc. of CVPR*, 9726–9735.
- Huang, F.; Zhang, L.; Fu, X.; and Song, S. 2024. Dynamic Weighted Combiner for Mixed-Modal Image Retrieval. In *Proc. of AAAI*, 2303–2311.
- Hurst, A.; Lerer, A.; Goucher, A. P.; Perelman, A.; Ramesh, A.; Clark, A.; Ostrow, A.; Welihinda, A.; Hayes, A.; Radford, A.; et al. 2024. Gpt-4o system card. *ArXiv preprint*.
- Karthik, S.; Roth, K.; Mancini, M.; and Akata, Z. 2024. Vision-by-Language for Training-Free Compositional Image Retrieval. In *Proc. of ICLR*.
- Levy, M.; Ben-Ari, R.; Darshan, N.; and Lischinski, D. 2024. Data Roaming and Quality Assessment for Composed Image Retrieval. In *Proc. of AAAI*, 2991–2999.
- Li, J.; Li, D.; Xiong, C.; and Hoi, S. C. H. 2022. BLIP: Bootstrapping Language-Image Pre-training for Unified Vision-Language Understanding and Generation. In *Proc. of ICML*, 12888–12900.
- Li, K.; Patel, O.; Viégas, F. B.; Pfister, H.; and Wattenberg, M. 2023. Inference-Time Intervention: Eliciting Truthful Answers from a Language Model. In *Proc. of NeurIPS*.
- Li, Z.; Chen, Z.; Wen, H.; Fu, Z.; Hu, Y.; and Guan, W. 2025. Encoder: Entity mining and modification relation binding for composed image retrieval. In *Proc. of AAAI*, 5101–5109.
- Liu, H.; Li, C.; Wu, Q.; and Lee, Y. J. 2023a. Visual Instruction Tuning. In *Proc. of NeurIPS*.
- Liu, S.; Ye, H.; Xing, L.; and Zou, J. Y. 2024a. In-context Vectors: Making In Context Learning More Effective and Controllable Through Latent Space Steering. In *Proc. of ICML*.
- Liu, Y.; Zhang, Y.; Cai, J.; Jiang, X.; Hu, Y.; Yao, J.; Wang, Y.; and Xie, W. 2025. Lamra: Large multimodal model as your advanced retrieval assistant. In *Proc. of CVPR*, 4015–4025.
- Liu, Z.; Luo, P.; Qiu, S.; Wang, X.; and Tang, X. 2016. DeepFashion: Powering Robust Clothes Recognition and Retrieval with Rich Annotations. In *Proc. of CVPR*, 1096–1104.
- Liu, Z.; Opazo, C. R.; Teney, D.; and Gould, S. 2021. Image Retrieval on Real-life Images with Pre-trained Vision-and-Language Models. In *Proc. of ICCV*, 2105–2114.
- Liu, Z.; Sun, W.; Hong, Y.; Teney, D.; and Gould, S. 2024b. Bi-directional training for composed image retrieval via text prompt learning. In *Proc. of WCACV*, 5753–5762.
- Liu, Z.; Sun, W.; Teney, D.; and Gould, S. 2023b. Candidate set re-ranking for composed image retrieval with dual multimodal encoder. *ArXiv preprint*.
- Maaten, L. v. d.; and Hinton, G. 2008. Visualizing data using t-SNE. *Journal of machine learning research*, 2579–2605.
- McGrath, T.; Kaphishnikov, A.; Tomašev, N.; Pearce, A.; Wattenberg, M.; Hassabis, D.; Kim, B.; Paquet, U.; and Kramnik, V. 2022. Acquisition of chess knowledge in AlphaZero. *Proceedings of the National Academy of Sciences*, e2206625119.

- Radford, A.; Kim, J. W.; Hallacy, C.; Ramesh, A.; Goh, G.; Agarwal, S.; Sastry, G.; Askell, A.; Mishkin, P.; Clark, J.; Krueger, G.; and Sutskever, I. 2021. Learning Transferable Visual Models From Natural Language Supervision. In *Proc. of ICML*, 8748–8763.
- Shankar, D.; Narumanchi, S.; Ananya, H.; Kompalli, P.; and Chaudhury, K. 2017. Deep learning based large scale visual recommendation and search for E-Commerce. *ArXiv preprint*.
- Singh, B.; and Davis, L. S. 2018. An Analysis of Scale Invariance in Object Detection SNIP. In *Proc. of CVPR*, 3578–3587.
- Stolfo, A.; Balachandran, V.; Yousefi, S.; Horvitz, E.; and Nushi, B. 2024. Improving Instruction-Following in Language Models through Activation Steering. In *Proc. of ICLR*.
- Sun, S.; Ye, F.; and Gong, S. 2023. Training-free zero-shot composed image retrieval with local concept reranking. *ArXiv preprint*.
- Sun, Z.; Jing, D.; Yang, G.; Fei, N.; and Lu, Z. 2025. Leveraging large vision-language model as user intent-aware encoder for composed image retrieval. In *Proc. of AAAI*, 7149–7157.
- Tang, X.; Wang, X.; Lv, Z.; Min, Y.; Zhao, W. X.; Hu, B.; Liu, Z.; and Zhang, Z. 2025a. Unlocking General Long Chain-of-Thought Reasoning Capabilities of Large Language Models via Representation Engineering. In *Proc. of ACL*.
- Tang, Y.; Zhang, J.; Qin, X.; Yu, J.; Gou, G.; Xiong, G.; Lin, Q.; Rajmohan, S.; Zhang, D.; and Wu, Q. 2025b. Reason-before-retrieve: One-stage reflective chain-of-thoughts for training-free zero-shot composed image retrieval. In *Proc. of CVPR*, 14400–14410.
- Tian, B.; Lyu, X.; Liu, M.; Wang, H.; and Li, A. 2025a. Why Representation Engineering Works: A Theoretical and Empirical Study in Vision-Language Models. *ArXiv preprint*.
- Tian, L.; Zhao, J.; Hu, Z.; Yang, Z.; Li, H.; Jin, L.; Wang, Z.; and Li, X. 2025b. CCIN: Compositional Conflict Identification and Neutralization for Composed Image Retrieval. In *Proc. of CVPR*, 3974–3983.
- Vo, N.; Jiang, L.; Sun, C.; Murphy, K.; Li, L.; Fei-Fei, L.; and Hays, J. 2019a. Composing Text and Image for Image Retrieval - an Empirical Odyssey. In *Proc. of CVPR*, 6439–6448.
- Vo, N.; Jiang, L.; Sun, C.; Murphy, K.; Li, L.; Fei-Fei, L.; and Hays, J. 2019b. Composing Text and Image for Image Retrieval - an Empirical Odyssey. In *Proc. of CVPR*, 6439–6448.
- Wei, J.; Wang, X.; Schuurmans, D.; Bosma, M.; Ichter, B.; Xia, F.; Chi, E. H.; Le, Q. V.; and Zhou, D. 2022. Chain-of-Thought Prompting Elicits Reasoning in Large Language Models. In *Proc. of NeurIPS*.
- Wen, H.; Song, X.; Chen, X.; Wei, Y.; Nie, L.; and Chua, T. 2024. Simple but Effective Raw-Data Level Multimodal Fusion for Composed Image Retrieval. In *Proc. of SIGIR*, 229–239.
- Wen, H.; Zhang, X.; Song, X.; Wei, Y.; and Nie, L. 2023. Target-guided composed image retrieval. In *Proc. of ACM MM*, 915–923.
- Wu, H.; Gao, Y.; Guo, X.; Al-Halah, Z.; Rennie, S.; Grauman, K.; and Feris, R. 2021. Fashion IQ: A New Dataset Towards Retrieving Images by Natural Language Feedback. In *Proc. of CVPR*, 11307–11317.
- Yang, Z.; Xue, D.; Qian, S.; Dong, W.; and Xu, C. 2024. LDRE: LLM-based Divergent Reasoning and Ensemble for Zero-Shot Composed Image Retrieval. In *Proc. of SIGIR*, 80–90.
- Zou, A.; Phan, L.; Chen, S.; Campbell, J.; Guo, P.; Ren, R.; Pan, A.; Yin, X.; Mazeika, M.; Dombrowski, A.-K.; et al. 2023. Representation engineering: A top-down approach to ai transparency. *ArXiv preprint*.